In: Atomic, Molecular and Optical Physics… ISBN: 978-1-60456-907-0
Editor: L.T. Chen, pp. 235-260 

*Chapter 6*

# FIBER BRAGG GRATINGS AND THEIR APPLICATIONS AS TEMPERATURE AND HUMIDITY SENSORS

***Qiying Chen*** [*] ***and Ping Lu***
Department of Physics and Physical Oceanography,
Memorial University of Newfoundland
St. John's, Newfoundland A1B 3X7, Canada

## Abstract

As an important waveguiding medium, optical fiber plays significant roles in optical communications, optoelectronics, and sensors. A new type of microstructure inscribed in the optical fibers, i.e., fiber Bragg gratings (FBGs), has received considerable attention in recent years. A FBG is a type of distributed Bragg reflector constructed in a short segment of optical fiber that reflects specific wavelengths of light and transmits all the other components. In this chapter, optical properties of FBGs will be reviewed first with the underlying physical mechanisms. Different techniques to fabricate FBGs will be illustrated with the comparison of their advantages and drawbacks. For their important sensing applications, FBGs as temperature and humidity sensors will be discussed. The FBG sensors exceed other conventional electric sensors in many aspects, for instance, immunity to electromagnetic interference, compact size, light weight, flexibility, stability, high temperature tolerance, and resistive to harsh environment. A novel approach to realize individual temperature or humidity measurement, and their simultaneous measurement will be demonstrated by the use of FBGs coated with different polymers. The polymer-coated FBGs indicate linear shifts in the Bragg resonance wavelengths of the gratings with the temperature changes. A polyimide-coated FBG is sensitive to humidity due to the unique hygroscopic properties of polyimide while an acrylate-coated FBG shows insensitivity to humidity. The experimental results are in good agreement with the theoretical analysis.

**Keywords:** Fiber Bragg grating (FBG), humidity sensing, temperature sensing, polymers.

[*] Corresponding author. E-mail: qiyingc@mun.ca; Phone: 1 709 737-8878; Fax: 1 709 737-8739.

# 1. Introduction

Guided wave optics is the forefront of research in optics nowadays. For modern applications, such as optical telecommunications and optical sensors, optical waveguides are the key components in which generation, modulation, propagation, and detection of light are governed by the principles of guided wave optics. An optical waveguide is a dielectric structure that transports energy at a wavelength in the infrared or visible portions of the electromagnetic spectrum [1]. Common waveguides used for optical communications are highly flexible fibers composed of nearly transparent dielectric materials. Charles Kao first suggested the possibility that low-loss optical fibers could be competitive with coaxial cable and metal waveguides for telecommunications applications in 1966 [2]. The commercial applications of optical fibers were not possible until 1970 when Corning Glass Work discovered an optical fiber with a loss less than the benchmark level of 10 dB/km [3,4].

With the increasing interests in the studies of all-fiber systems, fiber Bragg gratings (FBGs) have been applied in many photonic devices. A FBG is a type of distributed Bragg reflector constructed in a short segment of optical fiber that reflects specific wavelengths of light and transmits all the other components. A FBG can also be regarded as a fiber device with a periodic variation of the refractive index of the fiber core along the length of the fiber. The physical mechanism of inscribing the Bragg grating in a fiber is the photosensitivity of the fiber core. When a germanium-doped ($GeO_2$-doped) fiber is exposed to a high-intensity ultraviolet light, the refractive index of the fiber core is permanently changed [5]. The amount of change in the refractive index varies from $10^{-5}$ to $10^{-3}$. The phenomenon of the change in the refractive index of the fiber upon light irradiation is usually referred as photosensitivity. In 1978, Hill *et al.* first reported the photosensitivity phenomenon in optical fibers achieved by the interference between counter-propagating waves inside the fiber core [6]. A decade later, Meltz *et al*. obtained the first FBG which was imprinted in Ge-doped silica single mode fiber by transverse coherent 244 nm UV beams from a tunable excimer-pumped dye laser with a frequency-doubled crystal [7]. Since then, FBGs have been applied in optical communications and optical fiber sensor networks owing to their unique advantages and versatility as in-fiber devices. FBGs are now widely used in a variety of lightwave communication applications such as fiber laser [8, 9], fiber amplifier [10], fiber Bragg filter [11,12], wavelength division multiplexers/demultiplexers [13,14], and dispersion compensation [15]. On the other hand, FBGs have been used as excellent sensor elements for measuring many environmental parameters, including temperature, strain, bending, refractive index, pressure, and flow rate [16].

In the following part of this chapter, basic optical properties of FBGs will be briefly reviewed first together with their fabrication techniques followed by an overview of FBG sensors. The third part of this chapter will discuss FBG sensors for temperature and humidity measurements.

# 2. Properties of Fiber Bragg Gratings

## 2.1. Optical Properties

The fundamental properties of optical fibers and FBGs inscribed on the fibers have been discussed in several books and monographs [5, 17-21]. In this section, a brief review on the optical properties of FBGs will be given and details can be found from these references.

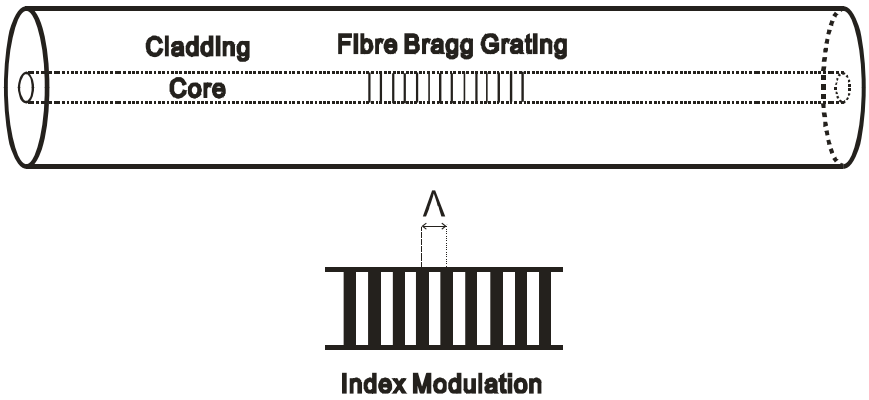


Figure 1. Illustration of a uniform fiber Bragg grating.

For a FBG consisting of a periodic modulation of the refractive index in the core of an optical fiber, the phase fronts are perpendicular to the fiber longitudinal axis and the grating planes are of a constant period, as illustrated in Fig. 1. Light propagating along the fiber core will interact with each grating plane, in which the Bragg condition is used for the discussion of the light propagation,

$$2\Lambda \sin\theta = n\lambda \,, \tag{1}$$

where $\Lambda$ is the spacing between the grating planes, $\theta$ is the angle between the incident light and the scattering planes, $\lambda$ is the light wavelength, and $n$ is an integer. In the case when the Bragg condition is not satisfied, the light reflected from each of the subsequent planes becomes progressively out of phase and will eventually disappear. Only when the Bragg condition is met, the contributions of reflected light from each grating plane add constructively in the backward direction to form a back-reflected peak with a center wavelength defined by the grating parameters, i.e., the Bragg wavelength.

The Bragg grating resonance condition is the requirement to satisfy both energy and momentum conservation, in which the energy conservation ($\hbar\omega_f = \hbar\omega_i$) requests that the frequency of the reflected radiation should be the same as that of the incident radiation while the momentum conservation implies that the incident wave vector, $\vec{k}_i$, plus the grating wave vector, $\vec{K}$, equal the wave vector of the scattered radiation $\vec{k}_f$,

$$\vec{k}_i + \vec{K} = \vec{k}_f \tag{2}$$

where the grating wave vector $\vec{K}$ has a direction normal to the grating plane with a magnitude $2\pi/\Lambda$.

The diffracted wave vector is equal in magnitude with opposite direction with regard to the incident wave vector. The momentum conservation condition can be simplified as the first –order Bragg condition

$$\lambda_B = 2n_{eff}\Lambda \tag{3}$$

where $\lambda_B$ is the Bragg grating wavelength, which is the center wavelength of the input light in the free space that will be back-reflected from the Bragg grating. $n_{eff}$ is the effective refractive index of the fiber core at the free-space centre wavelength.

For a uniform FBG inscribed in the core of an optical fiber with a refractive index $n_0$. The refractive index profile is [22]

$$n(x) = n_0 + \Delta n \cos\left(\frac{2\pi x}{\Lambda}\right) \tag{4}$$

where $\Delta n$ and $x$ are the amplitude of the induced refractive index perturbation and the distance along the fiber longitudinal axis, respectively. The reflectivity of a grating with constant modulation amplitude and period can be described as [22]

$$R(l,\lambda) = \frac{\Omega^2 \sinh^2(sl)}{\Delta k^2 \sinh^2(sl) + s^2 \cosh^2(sl)} \tag{5}$$

where $R(l,\lambda)$ is the reflectivity which is a function of the grating length $l$ and wavelength $\lambda$, $\Omega$ is the coupling coefficient, $\Delta k = k - \pi/\lambda$ is the detuning wave vector, $k = 2\pi n_0/\lambda$ is the propagation constant, and $s = \sqrt{\Omega^2 - \Delta k^2}$. The coupling coefficient $\Omega$ for the sinusoidal variation of index perturbation along the fiber axis has been found as

$$\Omega = \frac{\pi \Delta n \eta(V)}{\lambda} \tag{6}$$

where $\eta(V)$ is a function of the normalized frequency $V$ of the fiber that represents the fraction of the fiber mode power contained in the core, $\eta(V) \approx 1 - V^{-2}$. The normalized frequency $V$ can be expressed as [22]

$$V = \left(2\pi/\lambda\right) a \left(n_{co}^2 - n_{cl}^2\right)^{1/2} \tag{7}$$

where $a$ is the core radius, $n_{co}$ and $n_{cl}$ are the refractive indices of the core and cladding, respectively.

At the Bragg grating center wavelength, there is no wave vector detuning and Δk equals zero, the expression for the reflectivity becomes

$$R(l,\lambda) = \tanh^2(\Omega l). \tag{8}$$

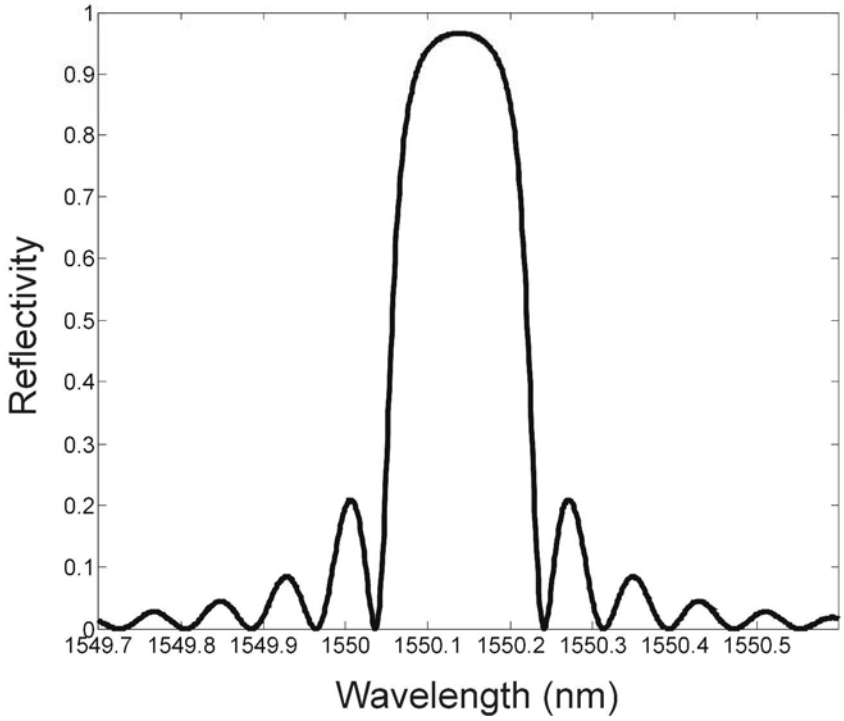


Figure 2. Simulation of the reflection spectrum of a FBG as a function of wavelength detuning.

The reflectivity increases with the change in the induced refractive index. It can also be found that the reflectivity increases with the increase in the length of the grating. Figure 2 gives a simulated reflection spectrum as a function of the wavelength detuning, in which the side lobes of the resonance are due to multiple reflections to and from opposite ends of the grating region.

A Bragg grating written in a highly photosensitive fiber exhibits a pronounced transmission feature on the short-wavelength side of the Bragg peak (Fig. 3). This feature is only observable in the transmission spectrum and only the main peak is visible in the reflection spectrum, which is due to the light leaving the fiber from the side. Radiation-mode coupling as a loss mechanism on core-mode transmission has been suggested to explain this phenomenon [23, 24]. For the cylindrical cladding-air interface, the transmission spectrum of

the Bragg grating consists of multiple sharp peaks that modulate the radiation-mode coupling. The light energy in the grating will be coupled to other modes at shorter wavelengths: some will be reflected or absorbed, and the others will be radiated away from the fiber. These interactions are seen as a series of many transmission dips in the spectrum at wavelengths that are shorter than the Bragg wavelength.

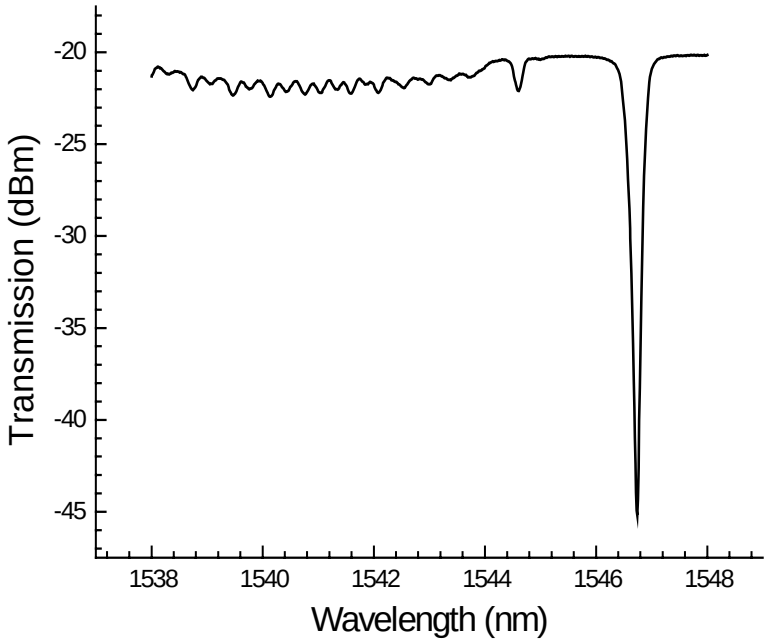


Figure 3. Transmission spectrum of a typical fiber Bragg grating exhibiting loss to radiation modes at the short-wavelength side.

## 2.2. Photosensitivity and Fabrication Techniques

As discussed in the previous section, photosensitivity in an optical fiber refers to a permanent change in the index of refraction of the fiber core when exposed to light of specific wavelength and intensity. Photosensitivity in optical fibers has significant importance in the fabrication of FBGs for applications in telecommunications and sensors.

After the first observation of weak changes ($\sim 10^{-6}$) in the index of refraction in germanosilica fibers by Hill *et al.* [6] in 1978, Meltz *et al.* showed that a strong index of refraction change occurred when a germanium-doped fiber was exposed to UV light close to the absorption peak of a germanium-related defect at a wavelength range of 240–250 nm [7]. Photosensitivity of optical fibers can be regarded as a measure of the amount of refractive index change in a fiber core. It is desirable to fabricate photoinduced devices in standard optical fibers for compatibility with existing systems, however, the standard single mode telecommunication fibers with a doping concentration of germanium around 3%, typically display weak index changes of $10^{-5}$, far below the expected value on the order of $10^{-4}$. Hydrogen loading (hydrogenation) [25-27], flame brushing [28], boron co-doping [29,30],

and short wavelength light source [31,32] have been used for enhancing the photosensitivity in silica optical fibers.

Bragg gratings have been written in many types of optical fibers using various methods. However, the mechanism of index change is not fully understood. Several models have been proposed for these photoinduced changes in the refractive index, for instance, the color center model [33,34], the dipole model [35], the compaction model [36], the stress-relief model [37-39]. The general idea from these theories is that the germanium–oxygen vacancy defects, Ge–Si or Ge–Ge, are responsible for the photoinduced index changes.

Direct optical inscription of high quality gratings into the cores of optical fibers has been actively pursued by many research laboratories and various techniques have been reported. Different FBG fabrication techniques can be classified as internal inscription and external inscription techniques. Adopted primarily during the earlier years [6], internally writing technique uses relatively simple experimental setup in which the standing wave inside the optical fiber photoimprints a Bragg grating with the same pattern as the standing wave. In recent years, the internal inscription technique has been superseded by the external inscription technique due to the intrinsic limitation of the internally written gratings. The reported externally written fabrication techniques can be categorized into four groups, i.e., interferometric technique, point-by-point exposure technique, phase mask technique, and most recently ultrashort pulse lasers technique.

The interferometric fabrication technique, the first external writing technique to inscribe Bragg gratings in photosensitive fibers, was demonstrated by Meltz *et al.* [7], in which two beams split from one UV light recombined to form an interference pattern and expose a photosensitive fiber inducing a refractive index modulation in the fiber core. Either amplitude-splitting or the wave-front-splitting interferometer has been used in the fabrication of FBGs.

The point-by-point exposure technique [40], which produces grating fringe one-by-one, is accomplished through UV light irradiation over consecutive steps. After each irradiation, either the fiber or the laser beam itself is translated in the axial direction of the fiber by a computer controlled translation stage. The advantage of this technique is that a laser beam of high intensity is obtained due to the focus of the laser beam with a flexibility to alter the Bragg grating parameters. The drawback of the point-by-point technique is that it is a time-consuming process. During the slow fabrication process, errors in the grating spacing due to thermal effects and/or small variations in the fiber's strain can occur, which limits the gratings to a very short length.

One of the most effective methods for inscribing Bragg gratings in photosensitive fiber is the phase-mask technique [41, 42]. This method employs a diffractive optical element, i.e., phase mask, to spatially modulate the UV writing beam. The phase-mask grating has a one-dimension surface-relief structure fabricated in a high-quality fused silica block transparent to the UV writing beam. The profile of the periodic gratings is chosen such that, when an UV beam is incident on the phase mask, the zero-order diffracted beam is suppressed to less than a few percent of the transmitted power. In addition, the diffracted plus and minus first orders are maximized to contain, typically, more than 35% of the transmitted power. A near-field fringe pattern is produced by the interference of the plus and minus first-order diffracted beams. The period of the fringes is one-half that of the mask. The interference pattern photoimprints a refractive-index modulation in the core of a photosensitive optical fiber placed in contact with or in close proximity immediately behind the phase mask. A

cylindrical lens may be used to focus the fringe pattern along the fiber core. The phase mask greatly reduces the complexity of the fiber grating fabrication system. The simplicity of using only one phase mask provides a robust and an inherently stable method for reproducing FBGs.

Recently, with the development of ultrafast laser technology, change of refractive index in transparent dielectrics with ultrashort laser pulses for photonic devices has been an interesting topic. Some published papers reported the use of femtosecond lasers to fabricate FBGs in commercial, non-photosensitized, and unhydrogenated fibers. These reported techniques include FBG inscription with standard or special phase masks [43,44] and direct point-by-point writing [45]. The wavelengths in the near-infrared region around 800 nm and ultraviolet (UV) around 248 nm have been used for FBG fabrication [45,46]. On the other hand, femtosecond lasers have also been demonstrated as a powerful tool in trimming FBGs to realize continuously tuning of the grating performance [47]. The ultrafast laser enhancement of photosensitivity response and modification of anisotropic index profile in silica fiber is a powerful technique to precise control of the performance of FBG devices for applications in optical filtering and polarization mode dispersion management.

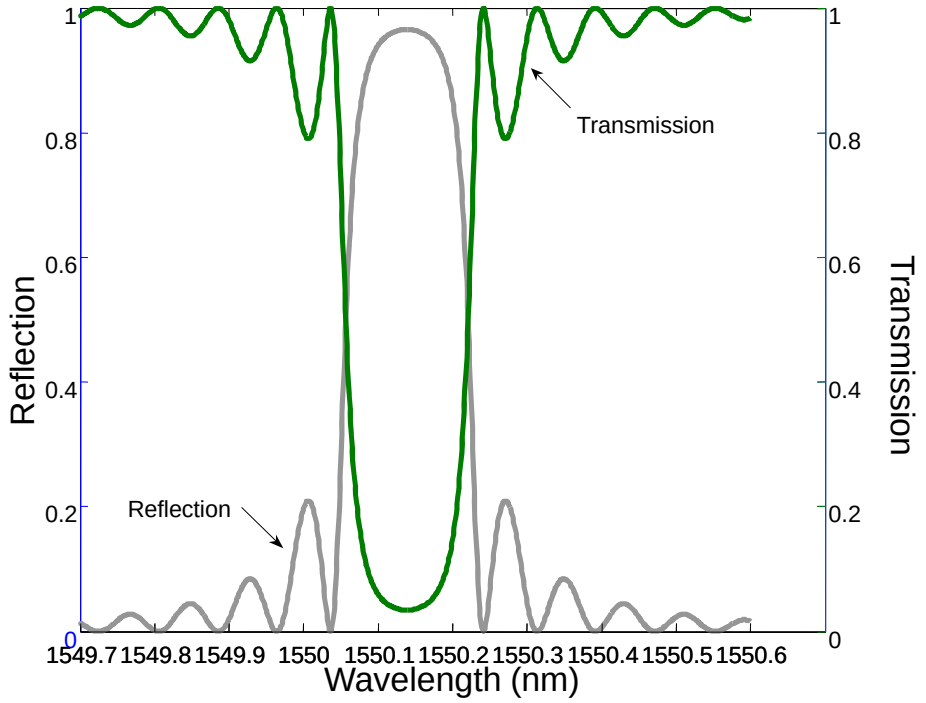


Figure 4. Simulated spectral response of a typical Bragg reflector with a uniform period.

According to the different grating pitch or tilt, fiber Bragg gratings can be classified into the common Bragg reflector, the blazed Bragg grating, and the chirped Bragg grating. The simplest and most frequently used FBG is the Bragg reflector, which has a constant pitch. A typical spectral response of a uniform period is shown in Fig. 4. The Bragg reflector can function as a narrowband transmission or reflection filter and sensor applications [48-51]. The

blazed grating has phase fronts tilted with respect to the fiber axis. The applications of blazed gratings are in mode conversion [52] and sensing field [53]. The chirped grating has an periodic pitch, displaying a monotonous increase in the spacing between grating planes. The applications of the chirped Bragg gratings are for dispersion compensation in high-bit-rate transmission systems [54, 55] and sensing elements [56-59].

## 3. Fiber Bragg Grating Sensors

Sensors based on FBGs have attracted considerable attention since the early stage of the discovery. FBG sensors exceed other conventional electric sensors in many aspects, for instance, immunity to electromagnetic interference, compact size, light-weight, flexibility, stability, high temperature tolerance, and resistance to harsh environment. Additional advantages of FBG sensors include very low insertion loss, narrowband wavelength reflection, linearity in response over many orders of magnitude and compatibility with the existing fiber optics system, especially their absolute wavelength-encoding of measurand information, making FBG sensors interrupt immune [60].

FBG sensors can measure many physical parameters, in which strain [61-64] and temperature [65, 66] measurements are the major fields of interest. Meltz and Morey propounded that the shift in the Bragg grating wavelength was mainly due to strain and temperature changes [67]. The strain response is induced due to both the fractional change in a grating period due to the physical elongation of the optical fiber and the change in fiber index due to photo-elastic effects. The thermal response is induced due to both the inherent thermal expansion of the fiber material and the temperature dependence of the refractive index. It is apparent that any shift in the Bragg wavelength is the sum of the strain and temperature factors. The sensing measurements of other measurands can be realized by transforming to the strain and temperature factors. FBG sensors used to measure humidity [68, 69], vibration [70], pressure [71-73], and refractive index [74-77], and salinity [78] have also been reported recently.

Various kinds of methods for temperature measurement have been developed by using optical fibers, which include blackbody radiation and pyrometry, absorption, intrinsic scattering, various forms of interferometry, and fluorescence based techniques [79], in addition to the newly emerged FBG techniques. Excellent reviews of optical fiber-based temperature sensing techniques can be found in Refs. [80,81]. Current research on optical fiber temperature sensing is focused on improving accuracy and/or the measurement range, and also reducing the cost. One particularly important topic is on identifying approaches to realize simultaneous measurement of multiple parameters, i.e., temperature and other environmental parameters. In many practical applications, it is required to monitor the temperature in order to achieve temperature compensation while measuring the environmental parameters, for example, flow rate, pressure, refractive index, and salinity.

Humidity is another important physical parameter for environmental control, industrial applications, and daily life. Lee *et al.* reviewed different types of optical humidity sensors [82]. One type of fiber-optic humidity sensors responses to the colorimetric interaction of materials immobilized on the surface of the fiber core or its cladding in the humidity-sensing section, in which the transmitted optical power changes as a function of the relative humidity due to the humidity-induced changes in the refractive indices of the materials. Kharaz *et al.*

reported an optical fiber humidity sensing system based on the colorimetric interaction of cobalt chloride with water molecules [83]. The use of a hydrophilic gel (agarose) deposited on the thinner zone of a biconically tapered single-mode optical fiber to achieve humidity measurement has been reported [84]. Gupta *et al.* discussed a fiber-optic humidity sensor based on the moisture-dependent absorption of light by using a phenol red doped polymethylmethacrylate (PMMA) film over a small portion of the core of the plastic clad silica fiber with a low refractive index [85]. Yeo *et al.* reported the use of a FBG together with a moisture sensitive polymer coating for humidity sensing [86]. Some polymer materials, such as polyimide, undergo volume expansion as a result of humidity absorption and desorption [87]. Once these polymers are coated on FBGs, the strain effects occur due to the volume changes of these coatings. Mrotek *et al.* discussed the diffusion of moisture through optical fiber coatings [88]. Other optical techniques have also been reported for humidity sensors, for example, changes in the incident light due to absorption [89], cooled mirror principles [90], and photo-acoustic technique [91]. Although optical sensors possess an advantage of high sensitivity, their drawbacks include hysteresis, large size, high power consumption for some optical fiber sensors other than in the forms of optical fibers, and especially missing of temperature compensation. The superiority of optical humidity sensors in tracking low moisture level has been noted [82].

As discussed above, FBGs respond to changes in both strain and temperature. It is necessary to discriminate these effects in order to reveal each physical parameter and various methods have been proposed. A practical approach is to use a reference grating or grating pairs [92, 93]. The reference grating or grating pairs, which is isolated from one parameter, e.g., strain, is placed near the sensor FBG. The reference grating can be on the same fiber as the sensor FBG [94]. Another method is to use two FBGs with a large difference in their Bragg wavelengths, which show different responses to the same measurands [95]. FBGs written on fibers of different diameters have also been proposed, which give different strain responses, while the temperature responses are the same [96,97]. A sensing head for simultaneous measurement of strain and temperature is demonstrated based on two Bragg gratings arranged in a twisted configuration [98]. By writing FBG with close wavelengths in undoped and boron doped fibers, different temperature sensitivities are obtained while the strain sensitivities remain the same [99]. In these reported techniques, it is necessary to use special fibers (specialty fibers with different doping elements, microstructured fibers, and photonic crystal fibers), complicated configurations (external lasers), or special spectroscopic techniques (fluorescence and interferometry) in order to distinguish temperature and strain, which result in bulky sensor systems targeting for the sole purpose of simultaneous measurement of temperature and strain only. Lu *et al.* reported an approach to resolve the cross-sensitivity between temperature and strain of FBGs [100], in which acrylate and polyimide polymers were used as the coating materials for different FBGs to achieve simultaneous measurement of axial strain and temperature. Since the standard FBG fabrication technique needs to strip the protective plastic coating off the fiber before FBG inscription and recoat a polymeric layer afterwards to protect the grating, the coating of FBGs with different polymeric materials proposed does not complicate the procedures or add extra cost in the FBG fabrication, which can be easily realized by fiber recoaters or dip coating technique. Furthermore, without additional optical devices or spectroscopic techniques, this approach provides one-fiber solution for multiple applications of FBGs in addition to resolve the cross-sensitivity of axial strain and temperature.

A large number of FBG sensors may be integrated at different locations along a single optical fiber or several fibers to form a quasi-distributed sensor [101-103]. The advantage of such kind of FBG array is that each FBG has a unique Bragg wavelength and can be individually interrogated. These FBG arrays can be fabricated with an arbitrary linear distance between the gratings, while the wavelength separation between the adjacent Bragg wavelengths is determined only by the wavelength shift of the neighboring higher and lower Bragg wavelengths.

Field applications of FBG sensors have also been reported [104-108]. FBG sensors possess a number of advantages for applications in spacecraft with embedded sensors that monitor the performance of reinforced carbon fiber composites as well as advanced testing of gas turbine engines [104]. There are numerous applications of FBG sensors for structural health monitoring in civil engineering, including monitoring of bridges [105], crack detection [106], and power transmission lines [107]. The FBG sensors can also be used in harsh environments [108].

# 4. Fiber Bragg Grating Temperature and Humidity Sensors

## 4.1. Theory

### 4.1.1. Fiber Bragg Grating Temperature Sensitivity

The Bragg grating resonance wavelength, $\lambda_B$, which is the center wavelength of light back reflected from a Bragg grating, depends on the effective index of refraction of the core ($n_{eff}$) and the periodicity of the grating ($\Lambda$) through the relation $\lambda_B = 2n_{eff}\Lambda$. The effective index of refraction, as well as the periodic spacing between the grating planes, will be affected by changes in temperature and strain. The shift in the Bragg grating wavelength $\Delta\lambda_B$ due to temperature and strain changes is given by [21]

$$\Delta\lambda_B = 2\left(\Lambda\frac{\partial n}{\partial T} + n\frac{\partial \Lambda}{\partial T}\right)\Delta T + 2\left(\Lambda\frac{\partial n}{\partial l} + n\frac{\partial \Lambda}{\partial l}\right)\Delta l. \tag{9}$$

The first term in Eqn. (9) represents the temperature effect on an optical fiber. The changes in the grating spacing and the index of refraction caused by thermal expansion result in a shift in the Bragg wavelength. This fractional wavelength shift for a temperature change $\Delta T$ may be written as [109]

$$\Delta\lambda_{B,T} = \lambda_B(\alpha + \zeta)\Delta T, \tag{10}$$

where $\alpha = (1/\Lambda)(\partial\Lambda/\partial T)$ is the thermal expansion coefficient of the fiber (~ $0.55\times10^{-6}$ °C$^{-1}$ for silica). The quantity $\zeta = (1/n)(\partial n/\partial T)$ represents the thermo-optic coefficient, which is $8.6\times10^{-6}$ °C$^{-1}$ for a germanium doped silica-core fiber. Clearly, the index change is by far

the dominant effect. From Eqn. (9), the expected temperature sensitivity of the FBG at 1550 nm is 0.0142 nm/°C.

### 4.1.2. Temperature and Humidity Sensitivity of Polyimide-coated Bragg Gratings

Using equation $\lambda_B = 2n_{eff}\Lambda$, the shift in the Bragg wavelength due to thermal expansion changes in the grating spacing and changes in the index of refraction can also be expressed as [109]

$$\frac{\Delta\lambda_B}{\lambda_B} = S_{RH}\Delta RH + S_T\Delta T = \left[\beta_{cf} - \hat{P}_e\left(\beta_{cf} - \beta_f\right)\right]\Delta RH + \left[\alpha_{cf} - \hat{P}_e\left(\alpha_{cf} - \alpha_f\right) + \zeta\right]\Delta T \tag{11}$$

where $S_{RH}$ and $S_T$ are the sensitivities to relative humidity and temperature, respectively. $\Delta RH$ and $\Delta T$ are the changes in the relative humidity and temperature accordingly. $\beta_i$ is the hygroscopic longitudinal expansion coefficient, which is zero for a bare fiber, and $\alpha_i$ is the thermal longitudinal expansion coefficient. The subscript stands for bare fiber ($i = f$) and coated fiber ($i = cf$). $\zeta$ is the thermo-optic coefficient of the fiber core, and $\hat{P}_e$ is the effective photoelastic coefficient of the coated fiber [108]

$$\hat{P}_e = \frac{n^2}{2}\left[P_{12} - \upsilon\left(P_{11}+P_{12}\right)\right] = 0.213 \tag{12}$$

where $P_{11}$ and $P_{12}$ are the components of the strain-optic tensor, $n$ is the index of refraction of the core, and $\upsilon$ is the Poisson's ratio. For a typical optical fiber $P_{11} = 0.113$, $P_{12} = 0.252$, $n = 1.482$, $\upsilon = 0.16$, and $\upsilon = -\varepsilon_{f,r} / \varepsilon_{f,z}$ where $\varepsilon_{f,r}$ and $\varepsilon_{f,z}$ are the radial and axial elastic fiber strains, respectively.

The temperature sensitivity $S_T$ can be expressed as

$$S_T = \alpha_{cf} - \hat{P}_e\left(\alpha_{cf} - \alpha_f\right) + \zeta \tag{13}$$

**Table 1. Properties of the fused silica fiber and the polyimide coating.**

| Parameter | Value |
|---|---|
| Thermal expansion coefficient $\alpha_f$ ($K^{-1}$) | $5\times10^{-7}$ |
| Thermal expansion coefficient $\alpha_c$ ($K^{-1}$) | $4\times10^{-5}$ |

| | |
|---|---|
| Thermo-optic coefficient $\xi$ ($K^{-1}$) | $(55 \pm 4.8) \times 10^{-7}$ |
| Young's modulus, E (Fiber) (GPa) | 72 |
| Young's modulus, E (coating) (GPa) | 2.45 |
| Poisson's ratio, ν (fiber) | 0.17 |
| Poisson's ratio, ν (coating) | 0.41 |
| Hygroscopic expansion coefficient $\beta_f$ ($\%RH^{-1}$) | 0 |
| Hygroscopic expansion coefficient $\beta_c$ ($\%RH^{-1}$) | $7 \times 10^{-5}$ |
| Thermal longitudinal expansion coefficient of coated fiber $\alpha_{cf}$ ($K^{-1}$) | $1.39 \times 10^{-6}$ |
| Hygroscopic longitudinal expansion coefficient of coated fiber $\beta_{cf}$ ($\%RH^{-1}$) | $1.58 \times 10^{-6}$ |

Table 1 lists some thermo-optic parameters of the fused silica fiber and the polyimide coating [78]. According to the table, the temperature sensitivity of the grating can be calculated to be $S_T = (6.70 \pm 0.48) \times 10^{-6}$ $K^{-1}$ $^oC^{-1}$. The temperature coefficient $K_T$, defined as $K_T = \Delta\lambda_B / \Delta T$, is $K_T = 0.0104$ nm/ °C at 1550 nm.

As we know that the hygroscopic longitudinal expansion coefficient of the bare fiber $\beta_f$ is zero, the relative humidity sensitivity $S_{RH}$ can be expressed as:

$$S_{RH} = \left(1 - \hat{P}_e\right) \beta_{cf} . \tag{14}$$

Following the parameters in Table 1, the relative humidity sensitivity $S_{RH}$ is $1.676 \times 10^{-6}$ $(\%RH)^{-1}$. The humidity coefficient $K_{RH}$, defined as $K_{RH} = \Delta\lambda_B / (\Delta RH)$, is $2.6 \times 10^{-3}$ nm/(%RH) at 1550 nm.

## 4.2. Experimental Details

A standard telecommunication optical fiber (SMF-28, Corning Inc.) was stored in a high hydrogen pressure environment (1900 psi) at room temperature for two weeks. Afterwards, the fiber was stored in a freezer at -70 °C before use. This process can prevent the hydrogen from diffusing out of the optical fiber. Hydrogen loading of a fiber satisfactorily enhances the photosensitivity of a fiber. A phase mask of 10 mm in length was used to write 1 cm FBG gratings onto the fiber with the laser irradiation from an ArF excimer laser (193 nm). The transmission spectrum of the FBG was monitored *in situ* during the laser exposure with a

white light source and an optical spectrum analyzer. Since the photosensitivity of an optical fiber also resulted in further changes of the central Bragg wavelength and the peak loss of the attenuation bands generated after fabrication when the hydrogen diffused out of the fiber, the FBG was baked at 150 °C overnight to eliminate the residual hydrogen and to stabilize the UV-induced index changes. The experimental setup for inscribing gratings is shown in Fig. 5.

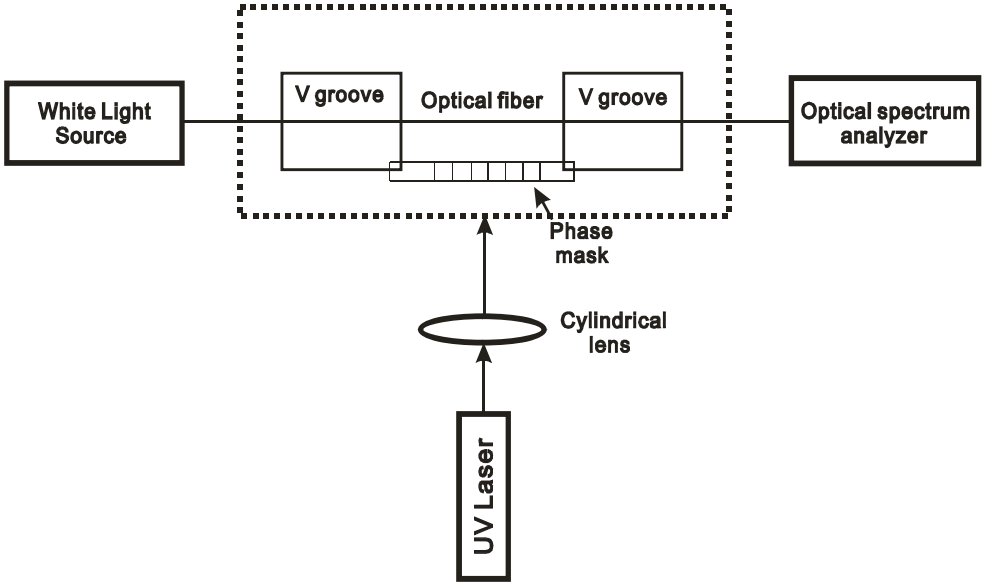


Figure 5. Schematic diagram of the fabrication of a fiber Bragg grating.

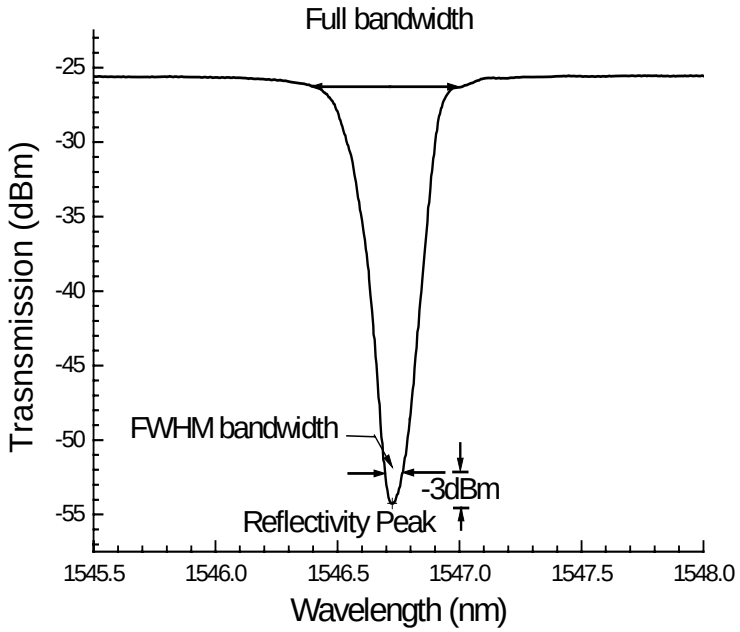


Figure 6. Transmission spectrum of a FBG at room temperature.

The transmission spectrum of a typical FBG is shown in Fig. 6. A broadband light travels through the optical fiber and enters into the FBG, from which one specific wavelength is reflected back by the FBG. Full width at half maximum (FWHM) is a parameter to characterize the bandwidths of laser beams or optical devices. For a strong FBG, it is normally measured at 3 dBm from the reflectivity peak.

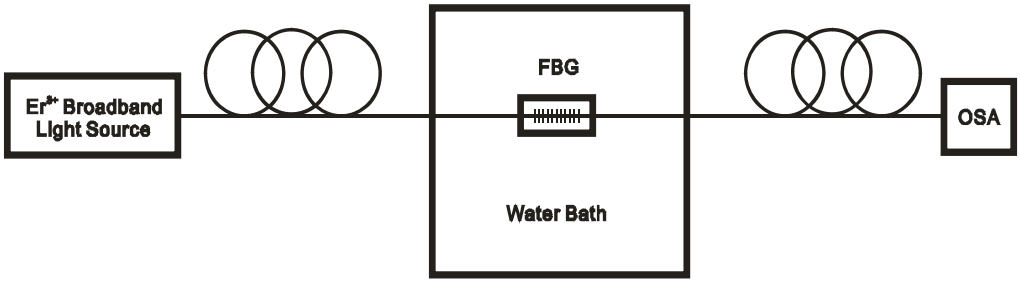


Figure 7. Schematic diagram of a temperature sensing measurement system.

Figure 7 illustrates the setup used to determine the temperature-induced shift in the resonance band of the FBG transmission spectrum. Light from a broadband light source (EBS-7210, MPB Communication, Inc.) was launched into one end of the fiber containing the grating and the transmission spectrum was recorded by an optical spectrum analyzer (ANDO AQ-6315E, Yokogawa Co.). The emission spectrum of the $Er^{3+}$ broadband source is shown in Fig. 8, which indicates an output in the wavelength range of 1525-1600 nm. The temperature of the grating was controlled by employing a microprocessor-controlled water bath (Precision 281). The FBG sample was immersed in the water bath for which the temperature has been kept constant for at least half an hour before measurement in order to ensure that the transmission spectrum of the FBG sample was immovable and the system was in a stable condition.

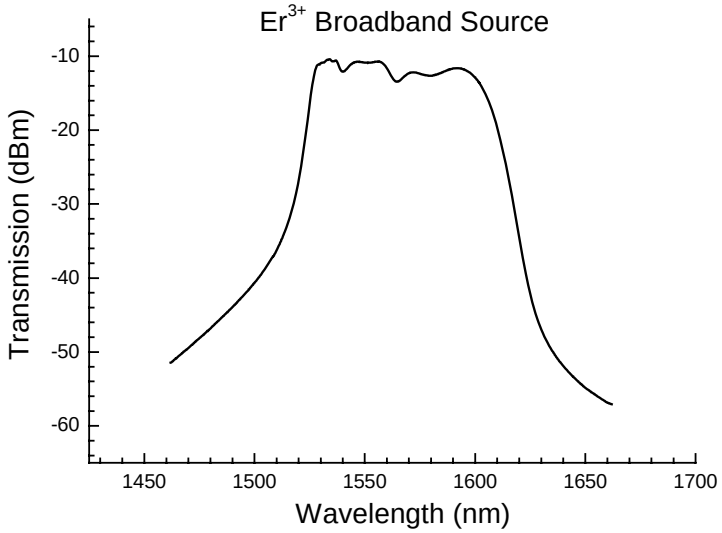


Figure 8. Emission spectrum of the $Er^{3+}$ broadband light source used in this study.

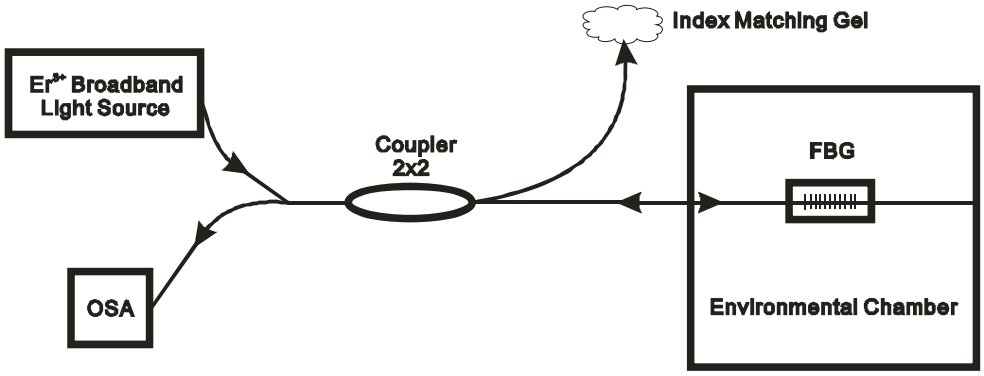


Figure 9. Schematic diagram of the humidity measurement system.

Once the FBG is inscribed onto the SMF-28 fiber, either acrylate or polyimide can be re-coated on the grating section using fiber recoaters or dip-coating method to protect the grating. The experimental setup used to characterize the humidity response of the sensor is shown in Fig. 9. The broadband light source was connected to the FBG sensor using a 2×2 fiber coupler. The reflected signal from the sensor was monitored using the optical spectrum analyzer. The polyimide-coated FBG sensor was stored inside an environmental chamber with controllable relative humidity. All experiments performed in this work were carried out at a room temperature of 20 $^{o}$C. Sufficient time was given to allow the test environment to stabilize before readings of the wavelength from the optical spectrum analyzer were recorded.

## 4.3. Temperature Sensing Response of Fiber Bragg Gratings

For testing the strong FBG used here, the water temperature in the water bath was first changed from 5 °C to 90 °C with a step of 5 °C, the temperature was then decreased from 90 °C to 35 °C with a step of 5 °C. At a temperature of 25 °C, the transmission spectrum is shown in Fig. 10.

For the heating process, the observed transmission spectra and the change of the Bragg resonance wavelength as a function of increasing temperature are shown in Figs. 11 and 12, respectively. The dependence of the red-shift of the resonance wavelength of the FBG on the increasing temperature was measured to be 0.0091 nm/ °C.

For the cooling process, the measured change of the Bragg resonance wavelength as a function of decreasing temperature is shown in Fig. 13. The shift in the Bragg wavelength with respect to the decreasing temperature was measured to be 0.0098 nm/ °C. The experimental results of the shift in the Bragg wavelength as a function of temperature are close to the expected value of 0.0142 nm/ °C for a FBG recoated with an acrylate coating. The difference of the temperature sensitivities between the experimental result and theoretical value is mainly due to a discrepancy between different coating materials induced thermal expansion coefficients of the cladding materials and the thermo-optic coefficients of different core materials. Results obtained from the heating and cooling processes demonstrated high repeatability of the temperature sensing measurement.

A general expression for the approximate FWHM bandwidth of a grating is given by [21]

$$\Delta\lambda = \lambda_B s\sqrt{\left(\frac{\Delta n}{2n_0}\right)^2 + \left(\frac{1}{N}\right)^2} \tag{15}$$

where $N$ is the number of the grating planes. The parameter $s$ is ~1 for strong gratings (for grating with near 100% reflection) whereas $s$ ~0.5 for weak gratings. The FWHM bandwidth of the FBG loss peak in the heating process is shown in Fig. 14 with a standard deviation of 4.3%, which indicates that the FWHM bandwidth is independent of the changing temperature.

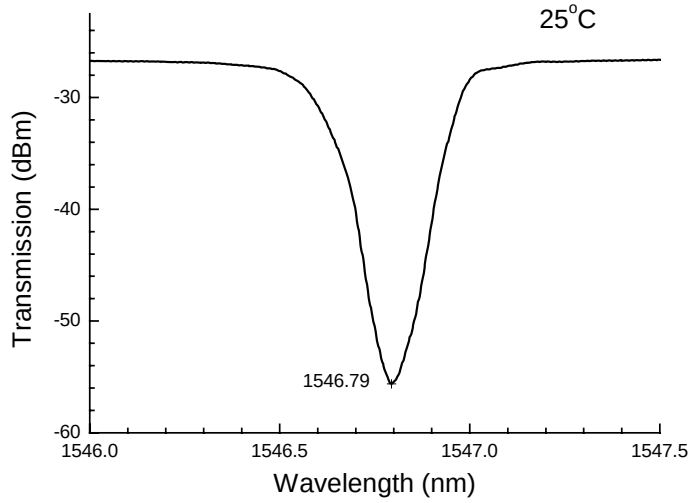


Figure 10. Transmission spectrum of a strong FBG at room temperature.

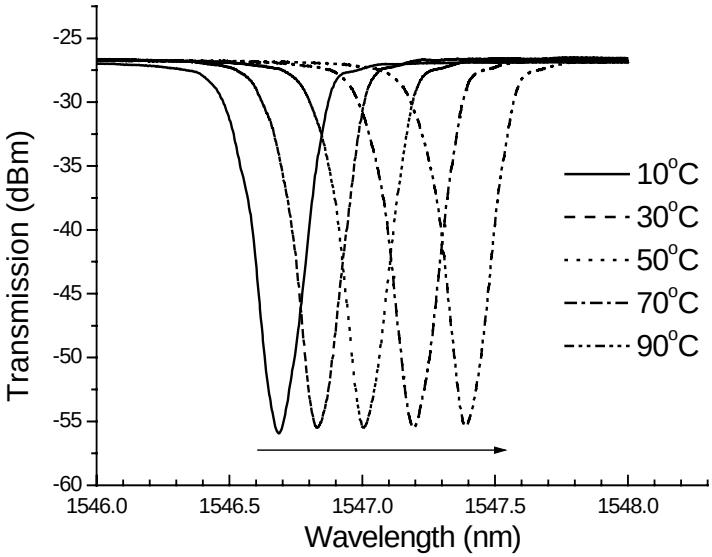


Figure 11. Transmission spectra of the FBG as a function of increasing temperature.

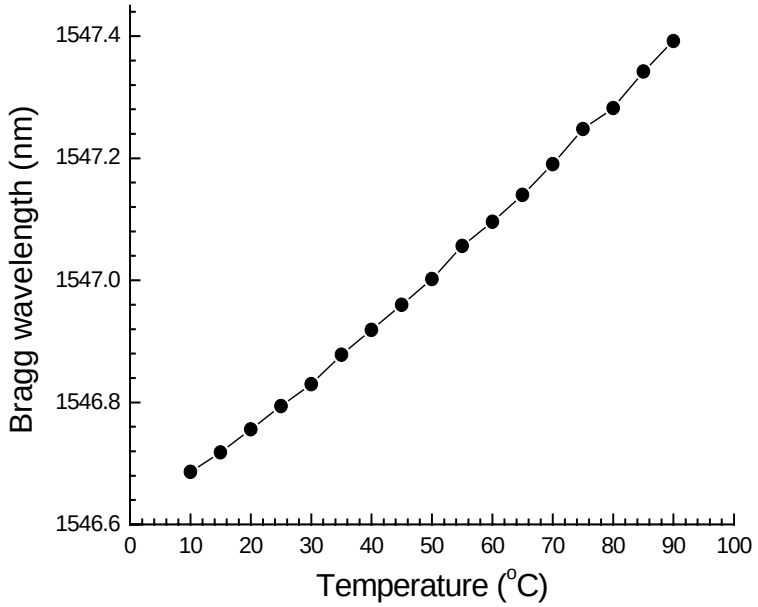


Figure 12. Bragg wavelength of the FBG as a function of increasing temperature.

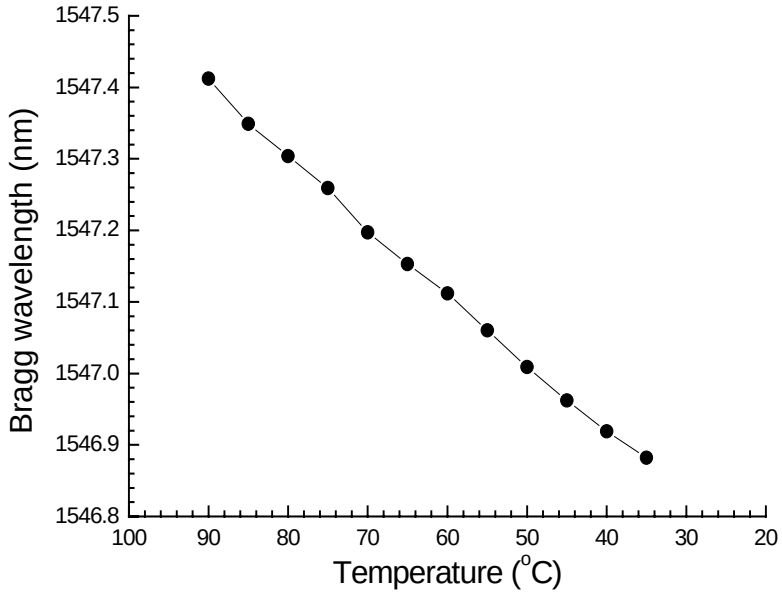


Figure 13. Bragg wavelength of the FBG as a function of decreasing temperature.

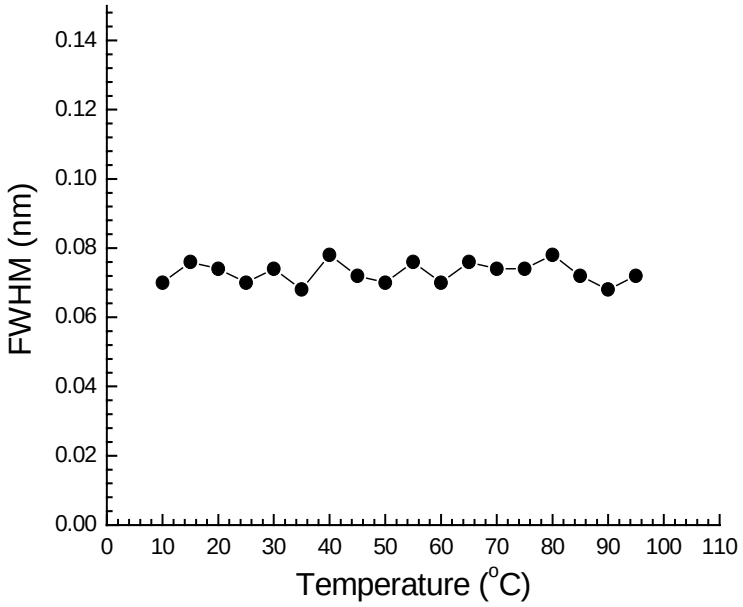


Figure 14. Change in the FWHM bandwidth of the FBG during heating process.

## 4.4. Humidity Sensing Response of Fiber Bragg Gratings

### 4.4.1. Humidity Sensing Response of a Polyimide-coated Fiber Bragg Grating

The polyimide-coated FBG was placed in the environmental chamber where the temperature was kept at 20 °C. At each fixed humidity setting, a reading was taken after the output signal from the optical spectrum analyzer had stabilized for 1 hour. The process was carried out three times to ensure reproducibility. As shown in Fig. 15, the data shows the behavior of the FBG spectral characteristics when the grating was exposed to different humidity conditions. From the figure, the Bragg wavelength shift was observed when the humidity in the test environment was varied from 13 %RH to 91 %RH. As the humidity level increased, the wavelength was found to shift toward the longer wavelength, which is consistent with the elongation of the FBG caused by the expansion of the polymer coating. This humidity change resulted in a wavelength shift of 0.22 nm.

Figure 16 shows the shifts of the Bragg wavelength versus relative humidity during three repeated tests. A linear regression was performed to establish the relationship between the wavelength shift due to the material expansion and the humidity level in the test chamber. The linear fitting reveals a linear dependence between the two parameters, which agrees well with the observations made by Kronenberg *et al*. [68] and Sager *et al*. [110], where the volume expansion of the polyimide film varies linearly with humidity. The humidity sensitivities of the FBG at 1550 nm were calculated to be 2.85, 2.62, and 2.60 pm/(%RH) respectively. The discrepancy among these test results may be ascribed to the incomplete adhesion between the silica surface and the polyimide layer due to the weak physical bonding at the interface between the fiber and the coating.

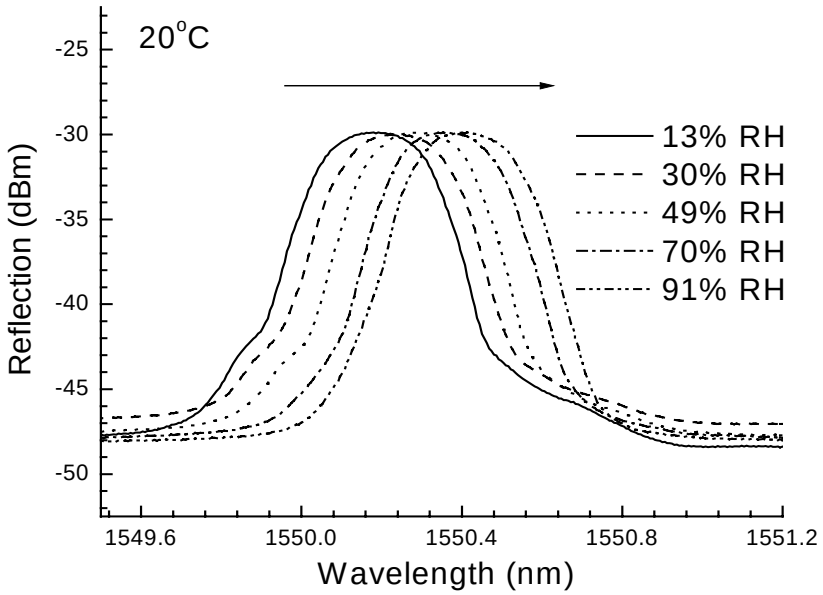


Figure 15. Reflection spectra of the polyimide-coated FBG at different relative humidities at room temperature.

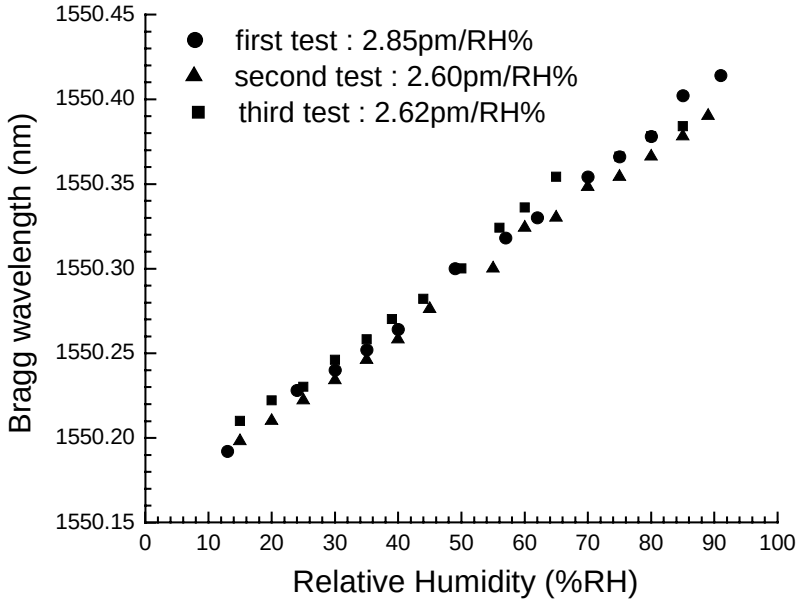


Figure 16. Bragg wavelength of the polyimide-coated FBG wavelength as a function of relative humidity in the environmental chamber.

Bare silica fibers are not sensitive to humidity. Polyimide polymers, however, are hygroscopic and will swell in aqueous media as the water molecules migrate into them. The swelling of the polyimide coating strains the fiber, which modifies the Bragg condition of the FBG and thus serves as the basis as the humidity sensor.

### 4.4.2. Humidity Sensing Response of an Acrylate-coated Fiber Bragg Grating

Following the same procedures mentioned above, FBG wavelength of an acrylate-coated FBG as a function of increasing and decreasing relative humidity were measured with the results shown in Figs. 17 and 18, respectively. The results in these two figures clearly indicate that the change of relative humidity will not change the center wavelength of the FBG at room temperature. The acrylate-coated FBG is therefore not sensitive to the change in relative humidity.

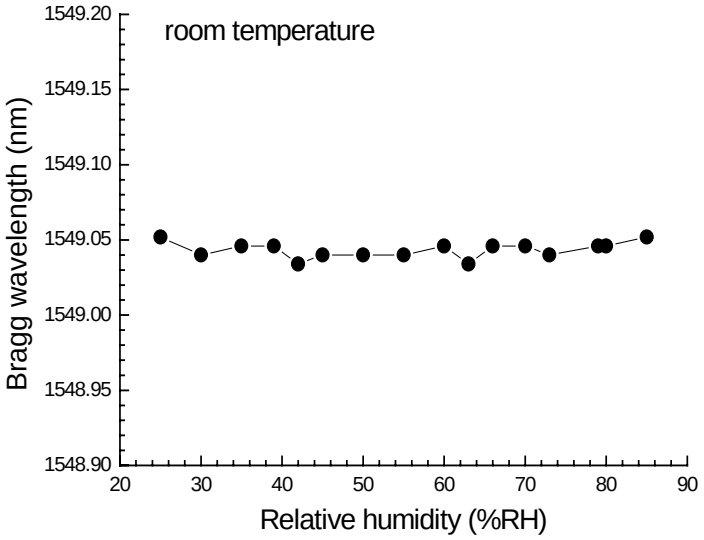


Figure 17. Bragg wavelength of the acrylate-coated FBG wavelength as a function of increasing relative humidity.

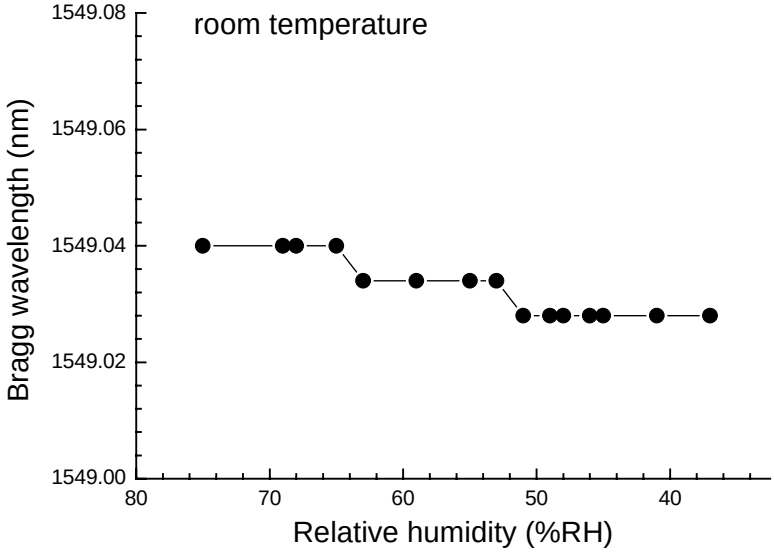


Figure 18. Bragg wavelength of the acrylate-coated FBG wavelength as a function of decreasing relative humidity.

## 5. Conclusions

Fiber Bragg gratings as temperature and humidity sensors have been reviewed and demonstrated, which possess many unique advantages over conventional techniques. Due to the nature of the fiber grating, it is possible to realize simultaneous measurement of these two parameters or to achieve quasi-distribution monitoring. Investigation on FBGs for applications in high temperature or harsh environment has been one of the research foci nowadays. For FBG humidity sensors, further research is needed for a systematic study of different polymer materials in order to identify materials with better performance as well as the sensing mechanisms including diffusion processes and response time.

### Acknowledgments

This work has been supported by the Natural Sciences and Engineering Research Council of Canada (NSERC), Canada Research Chairs Program, Canada Foundation for Innovation, the Province of Newfoundland and Labrador, and the Memorial University of Newfoundland.

**Reviewer:**

Yanfei Ding, Department of Physics and Physical Oceanography, Memorial University of Newfoundland, St. John's, NL A1B 3X7, Canada.

## References

[1] Snyder, A. W.; Love, J. D. *Optical Waveguide Theory*; Chapman and Hall: London, UK, 1983, 3-5.
[2] Kao, K. C.; Hockham, G. A. *Proc. IEE*, 1966, 113, 1151-1158.
[3] Keck, D. B.; Schultz, P. C.; Zimar, F. W. U. S. Patent 3, 737, 393.
[4] Kapron, F. P.; Keck, D. B.; Maurer, R. D. *Appl. Phys. Lett.* 1970, 17, 423-425.
[5] Iizuka, K. Elements of Photonics, Vol. II *For Fiber and Intergrated Optics*; Wiley-Interscience, New York, NY, 2002, 741.
[6] Hill, O.; Fujii, Y.; Johnson, D. C.; Kawasaki, B. S. *Appl. Phys. Lett*. 1978, 32, 647-649.
[7] Meltz, G.; Morey, W. W.; Glenn, W. H. *Opt. Lett.* 1989, 14, 823-825.
[8] Feng, X.; Tam, H. Y.; Wai, P. K. A. *Photon. Technol. Lett.* 2006, 18, 1088-1090.
[9] Liu, Y.; Chiang, K. S.; Chu, P. L. *Appl. Opt*. 2005, 44, 4822-4829.
[10] Liaw, S. K.; Dou, L.; Xu, A. *Opt. Exp.* 2007, 15, 12356-12361.
[11] Lausten, R.; Rochon, P.; Ivanov, M.; Cheben, P.; Janz, S.; Desjardins, P.; Ripmeester, J.; Siebert, T.; Stolow, A. *Appl. Opt*. 2005, 44, 7039-7042.
[12] Littler, I.; Rochette, M.; Eggleton, B. *Opt. Exp*. 2005, 13, 3397-3407.
[13] Bilodeau, F.; Johnson, D. C.; Thenault, S.; Malo, B.; Albert, J.; Hill, K. O. *IEEE Photon. Technol. Lett*. 1995, 7, 388-390.
[14] Dong, L.; Hua, P.; Birks, T. A.; Reekie, L.; Russell, P. St. J. *IEEE Photon Technol. Lett*. 1996, 8, 1656-1658.
[15] Sheu, L. G.; Chuang, K. P.; Lai, Y. *IEEE Photon. Technol. Lett*. 2003, 15, 939-941.

[16] López-Higuera, J. M. ed. *Handbook of Optical Fibre Sensing Technology*; John Wiley & Sons, Ltd: West Susses, England, 2002.
[17] Buck, J. A. *Fundamentals of Optical Fibers*; Wiley-Interscience: Hoboken, NJ, 2004.
[18] Bass, M. ed. Handbook of Optics Vol. IV. *Fiber Optics & Nonlinear Optics*, Second Edition; McGraw-Hill: New York, NY, 2001.
[19] Truesdale, C. M. Optical Fibers, in Waynant, R. W. and Ediger, M. N. ed. *Electro-Optics Handbook*, Second Edition, McGraw-Hill: New York, NY, 2000.
[20] Kashyap, R. *Fiber Bragg Gratings*; Academic Press: San Diego, CA, 1999.
[21] Othonos, A.; Kalli, K. *Fiber Bragg Gratings*; Artech House: Norwood, MA, 1999.
[22] Lam, D. K. W.; Garside, B. K. *Appl. Opt*. 1981, 20, 440-445.
[23] Mizrahi, V.; Sipe, J. E. *IEEE J. light. Technol*. 1993, 11, 1513-1517.
[24] Erdogan, T.; Sipe, J. E. *J. Opt. Soc. Am. A* 1996, 13, 296-313.
[25] Lemaire, P. J.; Atkins, R. M.; Mizrahi, V.; Reed, W. A. *Electron. Lett*. 1993, 29, 1191-1193.
[26] Atkins, R. M.; Lemaire, P. J.; Erdogan, T.; Mizrahi, V. *Electron. Lett*. 1993, 29, 1234-1235
[27] Awazu, K.; Kawazoe, H.; Yamane, M. *J. Appl. Phys.* 1990, 68, 2713-2718.
[28] Bilodeau, F.; Malo, B.; Albert, J.; Johnson, D. C.; Hill, K. O. *Opt. Lett*. 1993, 18, 953-955.
[29] Williams, D. L.; Ainslie, B. J.; Armitage, R.; Kashyap, R.; Campbell, R. *Electron. Lett.* 1993, 29, 45-47.
[30] Williams, D. L.; Ainslie, B. J.; Kashyap, R.; Maxwell, G. D.; Armitage, J. R.; Campbell, R. J.; Wyatt, R. *Proc. SPIE*, 1993, 2044, 55-68.
[31] Albert, J.; Malo, B.; Bilodeau, F.; Johnson, D. C.; Hill, K. O.; Hibino, Y.; Kawachi, M., *Opt. Lett*. 1994, 19, 387-389.
[32] Dyer, P. E.; Farley, R. J.; Gied, R.; Byron, K. C.; Reid, D. *Electron. Lett*. 1994, 30, 860-862.
[33] Atkins, R. M.; Mizrahi, V. *Electron. Lett*. 1992, 28, 1743-1744.
[34] Hand, D. P.; Russell, P. St. *J. Opt. Lett*. 1990, 15, 102-104.
[35] Bernandin, J. P.; Lawandy, N. M. *Opt. Commun*. 1990, 79, 194-199.
[36] Douay, M.; Xie, W. X.; Taunay, T.; Bernage, P.; Niay, P.; Cordier, P.; Poumellec, B.; Dong, L.; Bayon, J. F.; Poignant, H.; Delevaque, E. *IEEE J. light. Technol*. 1997. 15, 1329-1342.
[37] Fonjallaz, P. Y.; Limberge, H. G.; Salathe, R. P.; Cochet, F.; Leuenberger, B. *Opt. Lett.* 1995, 20, 1346-1348.
[38] Ky, N. H.; Limberge, H. G.; Salathe, R. P.; Cochet, F.; Dong, L. *Phys. Lett*. 1999, 74, 516-518.
[39] Limberge, H. G.; Fonjallaz, P. Y.; Salathe, R. P.; Cochet, F. *Appl. Phys. Lett*. 1996, 68, 3069-3071.
[40] Malo, B.; Hill, K. O.; Bilodeau, F.; Johnson, D. C.; Albert, J., *Electron. Lett*. 1993, 29, 1668-1669.
[41] Hill, K. O.; Malo, B.; Bilodeau, F.; Johnson, D. C.; Albert, *J. Appl. Phys. Lett*. 1993, 62, 1035-1037.
[42] Anderson, D. Z.; Mizrahi, V.; Erdogan, T.; White, A. E. *Proc. of the Conf. on Optical Fibre Communication, OFC'93,* Tech. Dig., 1993, 68.

[43] Dragomir, A.; Nikogosyan, D. N.; Zagorulko, K. A.; Kryukov, P. G.; Dianov, E. M.; *Opt. Lett.* 2003, 28, 2171-2173.
[44] Mihailov, S. J.; Smelser, C. W.; Grobnic, D.; Walker, R. B.; Lu, P.; Ding, H.; Unruh, J. *J. Light. Technol*. 2004, 22, 94-100.
[45] Martinez, A.; Dubov, M.; Khrushchev, I.; Bennion, I., *Electron. Lett*. 2004, 40, 1170-1172.
[46] Violakis, G.; Konstantaki, M.; Pissadakis, S. *IEEE Photon. Technol. Lett*. 2006, 18, 1182-1184.
[47] Chen, Q.; Chen, K. P.; Xu, W.; Nikumb, S. *Opt. Commun*. 2006, 259, 123-126.
[48] Kersey, A. D.; Davis, M. A.; Patrick, H. J.; LeBlanc, M.; Koo, K. P.; Askins, C. G.; Putnam, M. A.; Friebele, E. J. *IEEE J. light. Technol*. 1997, 15, 1442-1463.
[49] Ball, B.; More, W. W. *Opt. Lett.* 1992, 17, 420-422.
[50] Othonnos, A.; Alavie, A. T.; Serge, S. M.; Karr, S. E.; Measures, R. M. *Opt. Eng.* 1993, 32, 2841-2846.
[51] Alavie, A. T.; Karr, S. E.; Othonos, A.; Measures, R. M., *IEEE Photon. Technol. Lett.* 1993, 5, 1112-1114.
[52] Hill, K. O.; Bilodeau, F.; Faucher, S.; Malo, B.; Johnson, D. C. *Electron. Lett*. 1991, 27, 1548-1550.
[53] Laffont, G.; Ferdinand, P. *Meas. Sci. Technol*. 2001, 12, 765–770.
[54] Williams, J. A. R.; Bennion, I.; Sugden, K.; Doran, N. J. *Electron. Lett*. 1994, 30, 985-987.
[55] Kashyap, R.; Chernikov, S. V.; Mckee, P. F.; Taylor, J. R. *Electron. Lett*. 1994, 30, 1078-1080.
[56] Fallon, R. W.; Zhang, L.; Gloag, A.; Bennion, I. *Electron. Lett*. 1997, 33, 705-706.
[57] Putnam, M. A.; Williams, G. M.; Friebele, E. J. *Electron. Lett.* 1995, 31, 309-311.
[58] Leblanc, M.; Huang, S. Y.; Ohn, M.; Measures, R. M.; Guemes, A.; Othonos, A. *Opt. Lett*. 1996, 21, 1405-1407.
[59] Huang, S.; Leblanc, M.; Ohn, M. M.; Measures, R. M. *Appl. Opt.* 1995, 34, 5003-5009.
[60] Othonos, A.; Kalli, K. Fibre Bragg gratings Fundamentals and Applications in Telecommunications and Sensing, 1999, (Boston, MA: Artech House), 98-99
[61] Betz, D. C.; Thursby, G.; Culshaw, B.; Staszewski, W. J. *IEEE J. light. Technol*. 2006, 24, 1019-1026.
[62] Botsis, J.; Humbert, L.; Colpo, F.; Giaccari, P. *Opt. Laser. Eng.* 2005, 43, 491-510.
[63] Kersey, A. D.; Berkoff, T. A.; Morey, W. W. *Opt. Lett*. 1993, 18, 1370-1372.
[64] Fernandez, A.; Berghmans, F.; Brichard, B.; Megret, P.; Decreton, M.; Blondel, M.; Delchambre, A. *Meas. Sci. Technol.* 2001, 12, 1-4.
[65] Jung, J.; Nam, H.; Lee, B.; Byun, J. O.; Kim, N. S. *Appl. Opt.* 1999, 38, 2752-2754.
[66] Flockhart, G. M. H.; Maier, R. R. J.; Barton, J. S.; MacPherson, W. N.. Jones, J. D. C., Chisholm, K. E., Zhang, L., Bennion, I., Read, I. and Foote, P. D. *Appl. Opt.* 2004, 43, 2744-2751.
[67] Meltz, G.; Morey, W. W. *Proc. SPIE* 1991, 1516, 185-199.
[68] Kronenberg, P.; Rastogi, P. K.; Giaccari, P.; Limberger, H. G. *Opt. Lett.* 2002, 27, 1385-1387.
[69] Yeo, T. L.; Sun, T.; Grattan, K. T. V.; Parry, D.; Lade, R.; Powell, B. D. *IEEE Sensors J.* 2005, 5, 1082-1089.

[70] Dong, X.; Huang, Y.; Lang, K.; Zhang, W.; Kai, G.; Dong, X. Microw. *Opt. Tech. Lett*. 2004, 42, 474-476.
[71] Bock, W. J.; Urbańczyk, W. *Appl. Opt.* 1998, 37, 3897-3901.
[72] Hsu, Y. S.; Wang, L.; Liu, W.; Chiang, Y. J. *IEEE Photon. Technol. Lett*. 2006, 18, 874-876.
[73] Peng, B.; Zhao, Y.; Yang, J.; Zhao, M. *Measurement* 2005, 38, 176-180.
[74] Zhao, C.; Yang, X.; Demokan, M. S.; Jin, W. *IEEE J. Light. Technol*. 2006, 24, 879-883.
[75] Iadiciccoa, A.; Campopianoa, S.; Cutoloa, A.; Giordanob, M.; Cusanoa, A. *Sens. Actuators B,* 2006, 120, 231-237.
[76] Shu, X.; Gwandu, B. A. L.; Liu, Y.; Zhang, L.; Bennion, I. *Opt. Lett.* 2001, 26, 774-776.
[77] Iadicicco, A.; Campopiano, S.; Cutolo, A.; Giordano, M.; Cusano, A. *IEEE Photon. Technol. Lett.* 2005, 17, 1250-1252.
[78] Men, L.; Lu, P.; Chen, Q. *J. Appl. Phys*. 2008, 103, 053107.
[79] Wade, S. A.; Collins, S. F.; Baxter, G. W. *Appl. Phys. Lett.* 2003, 94, 4743-4756.
[80] Grattan, K. T. V.; Meggitt, B. T. Optical Fiber Sensor Technology; Chapman & Hall, London & Kluwer Academic, Dordrecht Netherlands, 1994/98/99, Vols. 1-4.
[81] Dakin, J.; Culshaw, B., Optical Fiber Sensors; Artech House, Boston, 1988/89/96, Vols. 1-3.
[82] Lee, C. Y.; Lee, G. B. *Sensors Lett.* 2005, 3, 1-14.
[83] Kharaz, A.; Jones, B. E.; *Sens. Actuators A* 1995, 46, 491-493.
[84] Bariáin, C.; Matías, I. R.; Arregui, F. J.; López-Amo, M. *Sens. Actuators B* 2000, 69, 127-131.
[85] Gupta, B. D.; Ratnanjali *Sens. Actuators B* 2001, 80, 132-135.
[86] Yeo, T. L.; Sun, T.; Grattan, K. T. V.; Parry, D.; Lade, R.; Powell, B. D.; *IEEE Sensors J*. 2005, 5, 1082-1089.
[87] Sager, K.; Schroth, A.; Nakladal, A.; Gerlach, G. Sens. Actuators A 1996, 53, 330-334.
[88] Mrotek, J. L.; Matthewson, M. J.; Kurkjian, C. R. *IEEE J. Light. Technol*. 2001, 19, 988-993.
[89] Schirmer, B.; Venzke, H.; Melling, A.; Edwards, C. S.; Barwood, G. P.; Gill, P.; Stevens, M.; Benyon, R.; Mackrodt, P. *Meas. Sci. Technol*. 2000, 11, 382-391.
[90] Sorli, B.; Pascal-Delannoy, F.; Giani, A.; Foucaran, A.; Boyer, A. *Sens. Actuators A* 2002, 100, 24-31.
[91] Bozóki, A.; Szakáll, M.; Mohácsi, Á.; Szabó, G.; Bor, Z., *Sens. Actuators B* 2003, 91, 219-226.
[92] Tang J. L.; Wang, J. N. *Sens. Transducers J.* 2006, 68, 597-605.
[93] Xu, M. G.; Reekie, L.; Chow Y. T.; Dakin, J. P. *Electron. Lett*. 1993, 29, 389-399.
[94] Song, M.; Lee, S. B.; Choi, S. S.; Lee, B. *Opt. Fiber Technol*. 1997, 3, 194-196.
[95] Xu, M. G., Archambault, J. L.; Reekie, L.; Dakin, J. P. *Electron. Lett*. 1994, 30, 1085-1087.
[96] James, S. W.; Dockney, M. L.; Tatam, R. P. *Electron. Lett.* 1996, 32, 1133-1134.
[97] Song, M.; Lee, B.; Lee, S. B.; Choi, S. S. *Opt. Lett*. 1997, 22, 790-792.
[98] Frazao, O.; Ferreira, L. J. Opt. A: *Pure Appl. Opt*. 2005, 7, 427-430.
[99] Cavaleiro, P. M.; Araujo, F. M.; Ferreira, L. A.; Santos, J. L.; Farahi, F. *IEEE Photon. Technol. Lett*. 1999, 11, 1635-1637.

[100] Lu, P.; Men, L.; and Chen, Q. 2008, *Appl. Phys. Lett*. **92**, 171112.
[101] Kersey, A. D.; Dandridge, A. *Proc. SPIE*, 1988, 985, 113-116.
[102] Berkoff, T. A.; Davis, M. A.; Bellemore, D. G.; Kersey, A. D. *Proc. SPIE*, 1995, 2444, 288-294.
[103] Askins, C. G.; Putnam, M. A.; Friebele, E. J. *Proc. SPIE,* 1995, 2444, 257-266.
[104] Friebele E. J.; Askins C. G.; Bosse A. B.; Kersey A. D.; Patrick H. J.; Pogue W. R.; Putnam M. A.; Simon W. R.; Tasker F. A.; Vincent W. S.; Vohra S. T. *Smart Mater. Struct.* 1999, 8, 813-838.
[105] Zhou, Z.; Graver, T. W.; Hsu, L.; Ou, J. *Pacific Science Review* 2003, 5, 116-121
[106] Okabe, Y.; Tanaka, N.; Takeda, N. *Smart Mater. Struct*. 2002, 11, 892–898.
[107] Bjerkan, L. *Appl. Opt.* 2000, 39, 554-560
[108] Wnuk, V. P.; Mendez, A.; Ferguson, S.; Graver, T. *Proc. SPIE*, 2005, 5758, 46-53.
[109] Meltz G. and Morey, W. W., *Proc. SPIE*, 1991, 1516, 185-199.
[110] Sager, K., Schroth, A., Nakladal, A., and Gerlach, G., *Sens. Actuators* 1996, 53, 330-334.